International Journal of Innovative Computing, Information and Control
Volume **8**, Number **1(A)**, January **2012**

ICIC International ©2012 ISSN 1349-4198
pp. **121–138**

MASTER-SLAVE CHAOS SYNCHRONIZATION USING AN ADAPTIVE DYNAMIC SLIDING-MODE NEURAL CONTROL SYSTEM

Chun-Fei Hsu[1,*], Chien-Jung Chiu[2] and Jang-Zern Tsai[2]

[1]Department of Electrical Engineering
Tamkang University
No. 707, Sec. 2, WuFu Rd., Hsinchu 30012, Taiwan
No. 151, Yingzhuan Rd., Danshui Dist., New Taipei City 25137, Taiwan
*Corresponding author: fei@ee.tku.edu.tw

[2]Department of Electrical Engineering
National Central University
No. 300, Jhongda Rd., Jhongli, Taoyuan County 32001, Taiwan
intel@ms63.hinet.net; jztsai@ee.ncu.edu.tw

Received August 2010; revised December 2010

Abstract. *Since chaotic systems are important nonlinear deterministic systems that display complex, noisy-like and unpredictable behavior, synchronizing chaotic systems have become an important issue in the engineering community. This paper proposes an adaptive dynamic sliding-mode neural control (ADSMNC) system composed of a neural controller and a switching compensator. The neural controller uses a radial basis function (RBF) network to online approximate an ideal dynamic sliding-mode controller, and the switching compensator is designed to guarantee system stability in the Lyapunov stability sense. Moreover, the online adaptive laws with variable learning rate are derived to speed up the convergence rates of the tracking error and controller parameters. Finally, the synchronization problem between two chaotic gyros based on the mater-slave scheme is studied. It is shown by the simulation results that the chaotic behavior of two nonlinear identical chaotic gyros can be synchronized by the proposed ADSMNC scheme after learning of the controller parameters.*

Keywords: Adaptive control, Neural control, Sliding-mode control, Variable learning rate

1. **Introduction.** It is well known that sliding-mode control (SMC), which is one of effective nonlinear robust control approaches, can provide system dynamics with an invariance property to uncertainties once the system dynamics is controlled in the sliding mode [1-3]. However, the SMC strategy usually suffers from large control chattering caused by a switching function in the control law. It may wear mechanism coupling and excite unmodelled system dynamics. A common method to improve the chattering is to replace the switching function by the saturation function. A trade-off problem between chattering and control accuracy arises [2]. To tackle this problem, among several kinds of modern SMC schemes, the dynamic sliding-mode control (DSMC) system is an effective control scheme for eliminating chattering [4,5]. The additional dynamics in the DSMC system can be considered as compensators designed for improving sliding-mode stability. Meanwhile, since DSMC uses an integration method to obtain practical control effort, the chattering phenomenon can be improved effectively.

Though favorable control performance can be achieved by using the SMC and DSMC systems, they need exact dynamic characteristics of controlled plants to design the control

law. To tackle this problem, many intelligent control schemes which don not need to know the system dynamics have been developed [6-12]. The most important feature of these intelligent control schemes is the self-learning ability that neural networks are used to approximate arbitrary linear or nonlinear mappings through online learning algorithms without requiring preliminary offline tuning. Convergence analysis of most of the learning algorithms was derived based on the Lyapunov stability theorem or the gradient decent method.

Radial basis function (RBF) networks are characterized by a simple structure with rapid computation time and superior adaptive performance. There have been considerable interests in exploring the applications of RBF network to deal with the non-linearity and uncertainty in control systems [13-16]. Though these RBF-based intelligent control schemes can achieve satisfied control performance through online learning algorithms, how to determine the learning rates of parameter adaptation laws usually requires some time-consuming trial-and-error tuning procedures. For a small learning rate, convergence of tracking error and controller parameters can be easily guaranteed, but with slow convergence speed. If the learning rate is too large, the parameter adaptation laws may lead to instability of the control systems.

To attack this problem concerning the learning rates of the parameter adaptation laws, a variable learning rate is studied [17-20]. In [17,18], a discrete-type Lyapunov function was utilized to determine the learning-rate parameters of the adaptation laws. However, exact calculation of the Jacobian term associated with the system is not feasible due to the unknown system dynamics. Wai and Tu [19] used a genetic algorithm to determine the learning-rate parameters of the adaptation laws; however, the computation loading is heavy and their scheme lacks real-time adaptation ability. Compared with the genetic algorithm, Lin et al. [20] used a particle swarm optimization to deal with the same problem. The particle swarm optimization algorithm has a quick convergent ability to make it become popular in many applications. However, the system stability can not be guaranteed and also lacks real-time adaptation ability.

Recently, synchronization among chaotic dynamical systems has received a great deal of interest among scientists from various fields [21-23]. Until now, many different methods have been applied theoretically and experimentally to synchronize chaotic systems. Yau [24] proposed a nonlinear rule-based controller for chaos synchronization. However, the fuzzy rules should be pre-constructed by a time-consuming trial-and-error tuning procedure to achieve the required performance. Poursamad and Davaie-Markazi [25] proposed a robust adaptive fuzzy controller with a switching compensator to ensure system's stability; however, the switching compensator required the bound of the system uncertainty and it will cause chattering phenomena. The adaptive control techniques are applied to chaos synchronization in [26-28]; however, these adaptive control schemes require the structural knowledge of the chaotic dynamic functions.

In this paper, an adaptive dynamic sliding-mode neural control (ADSMNC) system is proposed to synchronize two nonlinear identical chaotic gyros via the DSMC approach. The proposed ADSMNC system is composed of a neural controller and a switching compensator. Even though the plant is unknown, the proposed ADSMNC system can use the updating rules to adjust the controller parameters. To guarantee the convergence of tracking errors, an analytical method based on a discrete-type Lyapunov function is proposed to determine the conditions on learning rates of the parameter adaptation laws. Finally, in the simulation study, it is shown that the proposed ADSMNC system can drive the slave gyro system to synchronize the master gyro system with rapid convergence of the tracking error and without the chattering phenomena.

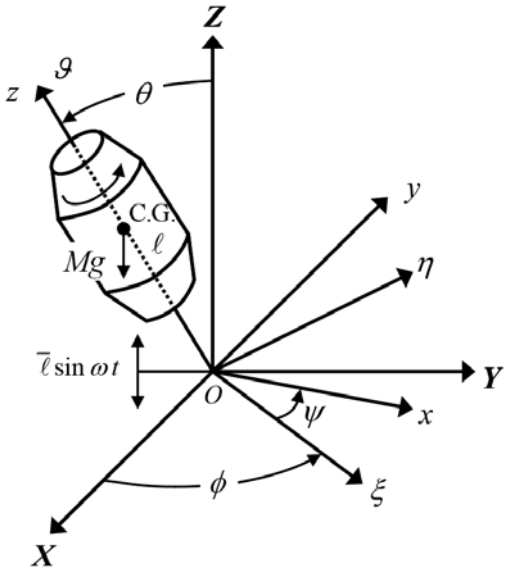

FIGURE 1. A schematic diagram of the symmetric gyro system

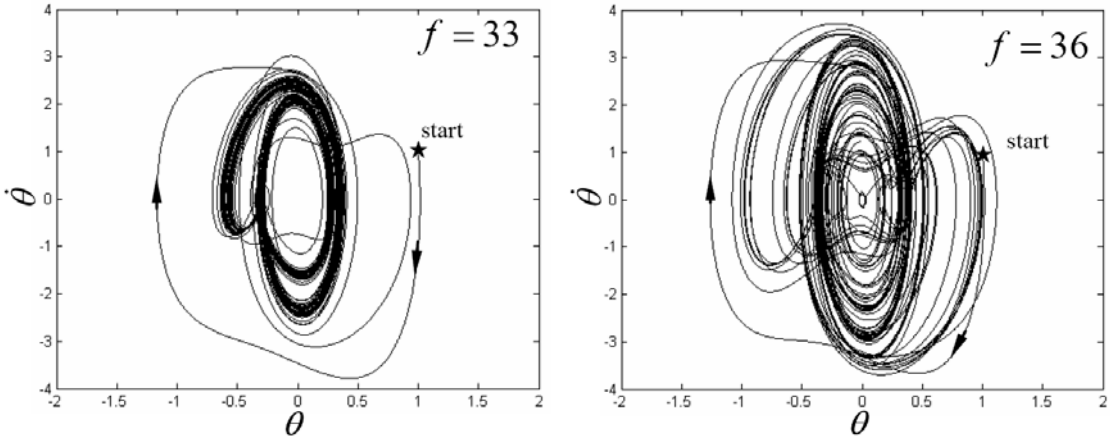

(a) (b)

FIGURE 2. Uncontrolled chaotic trajectories for different system parameters

2. **Problem Formulation and DSMC Design.** A gyroscope is a device for measuring or maintaining orientation based on the principle of conservation of angular momentum [21]. Usually, a gyroscope is mounted on the axis of rotation of the wheels. A schema of a symmetric gyro with linear-plus-cubic damping system is shown in Figure 1 where the attitude of the gyro mounted on a vibrating base are described by Euler's angles θ (nutation), ϕ (precession) and ψ (spin). The Lagrangian of the symmetric gyro can be described as follows:

$$L = \frac{1}{2}I_1(\theta^2 + \dot{\phi}^2 \sin^2\theta) + \frac{1}{2}I_3(\dot{\phi}\cos\theta + \dot{\psi})^2 - M_g(\ell + \bar{\ell}\sin\omega t)\cos\theta \tag{1}$$

where I_1 and I_3 are the polar and equatorial moments of inertia of the symmetric gyro, respectively, M_g is the gravity force, $\bar{\ell}$ is the amplitude of the external excitation disturbance, and ω is the frequency of the external excitation disturbance. Then, the dynamic

model of the symmetric gyro with linear-plus-cubic damping is given as [21].

$$\ddot{\theta} + \left(\frac{\beta_\Phi}{I_1}\right)^2 \frac{(1-\cos\theta)^2}{\sin^3\theta} - \frac{M_g\bar{\ell}}{I_1}\sin\theta + \frac{D_1}{I_1}\dot{\theta} + \frac{D_2}{I_1}\dot{\theta}^3 = \frac{M_g\bar{\ell}}{I_1}\sin\omega t\sin\theta \tag{2}$$

where $\beta_\Phi = \partial L/\partial\dot{\phi}$, D_1 and D_2 are positive constants. Equation (2) can be rewritten as

$$\ddot{\theta} + \alpha^2\frac{(1-\cos\theta)^2}{\sin^3\theta} - \beta\sin\theta + \gamma_1\dot{\theta} + \gamma_2\dot{\theta}^3 = f\sin\omega t\sin\theta \tag{3}$$

where θ is the angle, $f\sin\omega t$ is the parametric excitation, $\gamma_1\dot{\theta}$ and $\gamma_2\dot{\theta}^3$ are the linear and nonlinear damping, respectively, and $\alpha^2\dfrac{(1-\cos\theta)^2}{\sin^3\theta} - \beta\sin\theta$ is a nonlinear resilience force. The open-loop system behavior was simulated with $\alpha^2 = 100$, $\beta = 1$, $\gamma_1 = 0.5$, $\gamma_2 = 0.05$ and $\omega = 2$ for observing the chaotic unpredictable behavior. The time responses of the uncontrolled chaotic gyro with initial condition $(1, 1)$ with $f = 33$ and $f = 36$ are shown in Figures 2(a) and 2(b), respectively. It is shown the uncontrolled chaotic gyro has different types of trajectories for different system parameters.

Generally, the two chaotic systems in synchronization are called the drive (master) system and response (slave) system, respectively. In the chaos synchronization problem, it is required that the slave system can track the trajectories of the master system. Consider two coupled chaotic gyros systems as [21].

Master system:

$$\ddot{x} = f_x\sin\omega t\sin x - \alpha^2\frac{(1-\cos x)^2}{\sin^3 x} + \beta\sin x - \gamma_1\dot{x} - \gamma_2\dot{x}^3 = g_x \tag{4}$$

where $g_x = f_x\sin\omega t\sin x - \alpha^2\dfrac{(1-\cos x)^2}{\sin^3 x} + \beta\sin x - \gamma_1\dot{x} - \gamma_2\dot{x}^3$.

Slave system:

$$\ddot{y} = f_y\sin\omega t\sin y - \alpha^2\frac{(1-\cos y)^2}{\sin^3 y} + \beta\sin y - \gamma_1\dot{y} - \gamma_2\dot{y}^3 + u = g_y + u \tag{5}$$

where $g_y = f_y\sin\omega t\sin y - \alpha^2\dfrac{(1-\cos y)^2}{\sin^3 y} + \beta\sin y - \gamma_1\dot{y} - \gamma_2\dot{y}^3$ and u is the control input. If uncertainties occur, i.e., the system parameters deviate from their nominal values or an coupling term is added into the system, the two coupled chaotic gyros systems can be modified as

$$\ddot{x} = g_x + \Delta g_x \tag{6}$$

and

$$\ddot{y} = g_y + \Delta g_y + u + F \tag{7}$$

where Δg_x and Δg_y denote the system uncertainties of master system and slave system, respectively, and F denotes the coupling term. The control objective of the two coupled chaotic gyro systems is for different initial conditions of the master and slave systems, and the coupling term in the slave system, the two coupled system, i.e., the master system (4) and the slave system (5), are synchronized by designing an appropriate signal control input u. To achieve the control objective, the tracking error is defined as

$$e = x - y. \tag{8}$$

From Equations (6)-(8), the error dynamic equation can be obtained as

$$\ddot{e} = g_x - g_y - u + \Delta g_x - \Delta g_y - F = g_x - g_y - u + w \tag{9}$$

where the lumped uncertainty w is defined as $w = \Delta g_x - \Delta g_y - F$.

It is well known the major advantage of SMC and DSMC systems is their insensitivity to parameter variations and external disturbance once the system trajectory reaches and then stays on the sliding surface. The sliding surface is defined as

$$s = \dot{e} + a_1 e + a_2 \int_0^t e(\tau) d\tau \tag{10}$$

where a_1 and a_2 are positive constants, and a dynamic sliding surface is defined as

$$\varsigma = \dot{s} + b_1 s + b_2 \int_0^t s(\tau) d\tau \tag{11}$$

where b_1 and b_2 are positive constants. Differentiating Equation (11) with respect to time and using Equations (9) and (10) obtain

$$\begin{aligned} \dot{\varsigma} &= \ddot{s} + b_1 \dot{s} + b_2 s \\ &= \dot{g}_x - \dot{g}_y - \dot{u} + \dot{w} + (a_1 + b_1)\ddot{e} + (a_2 + a_1 b_1 + b_2)\dot{e} \\ &\quad + (a_2 b_1 + a_1 b_2) e + a_2 b_2 \textstyle\int_0^t e(\tau) d\tau \\ &= \dot{g}_x - \dot{g}_y - \dot{u} + \dot{w} + c_1 \ddot{e} + c_2 \dot{e} + c_3 e + c_4 \textstyle\int_0^t e(\tau) d\tau \end{aligned} \tag{12}$$

where $c_1 = a_1 + b_1$, $c_2 = a_2 + a_1 b_1 + b_2$, $c_3 = a_2 b_1 + a_1 b_2$ and $c_4 = a_2 b_2$. The ideal DSMC system is given as

$$u_{dsmc} = \int_0^t \dot{u}_{dsmc}(\tau) d\tau \tag{13}$$

$$\dot{u}_{dsmc} = \dot{g}_x - \dot{g}_y + c_1 \ddot{e} + c_2 \dot{e} + c_3 e + c_4 \int_0^t e(\tau) d\tau + W \operatorname{sgn}(\varsigma) \tag{14}$$

where W is a given positive constant with the assumption $|\dot{w}| \leq W$. Substituting Equation (14) into Equation (12) yields

$$\dot{\varsigma} = \dot{w} - W \operatorname{sgn}(\varsigma). \tag{15}$$

Consider the Lyapunov function candidate in the following form as

$$V_1 = \frac{1}{2}\varsigma^2. \tag{16}$$

Differentiating Equation (16) with respect to time and using Equation (15) obtains

$$\begin{aligned} \dot{V}_1 &= \varsigma\dot{\varsigma} = \dot{w}\varsigma - W|\varsigma| \\ &\leq |\dot{w}|\,|\varsigma| - W|\varsigma| \\ &= -(W - |\dot{w}|)\,|\varsigma| \leq 0. \end{aligned} \tag{17}$$

If the state trajectory stays on the dynamic sliding surface, i.e., $\dot{\varsigma} = \ddot{s} + b_1 \dot{s} + b_2 s = 0$, then it will asymptotically reach the sliding surface $s = 0$. Hence, after transient period, we can approximately have $s = 0$. Moreover, if $\dot{s} = \ddot{e} + a_1 \dot{e} + a_2 e = 0$, by choosing the values of a_1 and a_2 properly, the desired system dynamics such as setting time can be easily designed by the second-order system. Then, the control law of the DSMC system in Equation (14) can guarantee the stability in the Lyapunov sense [1,4]. Since the dynamics is usually nonlinear and a precise model is difficult to be obtained, the ideal DSMC system is difficult to be implemented.

3. **Design of the ADSMNC System.** To efficiently and precisely control the synchronization, an adaptive dynamic sliding-mode neural control (ADSMNC) system is proposed as shown in Figure 3, where the controller output is defined as

$$\dot{u}_{adsc} = \dot{u}_{nc} + \dot{u}_{sc}. \tag{18}$$

The neural controller $\dot{u}_{nc}$ uses a RBF network to approximate the ideal dynamic sliding-mode controller $\dot{u}_{dsmc}$ in Equation (14), and the switching compensator $\dot{u}_{sc}$ is designed to

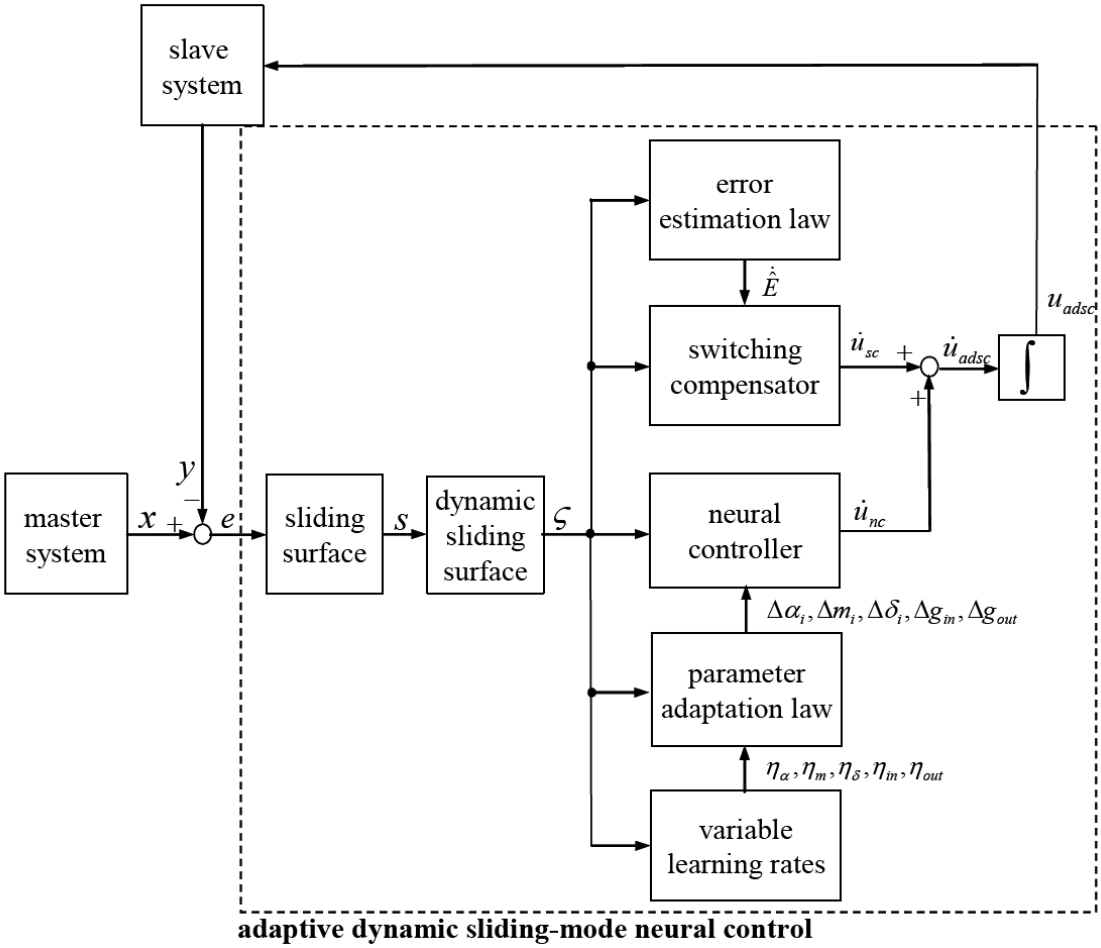

FIGURE 3. Block diagram of the ADSMNC system for chaos synchronization

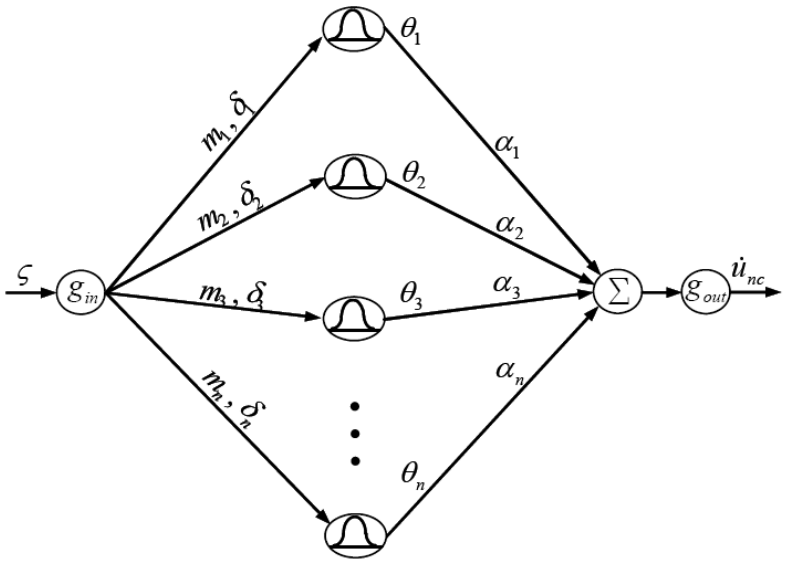

FIGURE 4. Structure of the RBF network

cope with the influence of residual approximation error introduced by the neural controller. The used RBF network is shown in Figure 4, and the output of the RBF network with n

hidden neurons is given by

$$\dot{u}_{nc} = g_{out}\left[\sum_{i=1}^{n}\alpha_i\theta_i(g_{in}\varsigma, m_i, \delta_i)\right] \tag{19}$$

where g_{in} and g_{out} are the scaling factors of the input and output variables, respectively; α_i represents the connection weights between the hidden layer and the output layer; and θ_i represents the firing weight of the i-th hidden neuron given as

$$\theta_i(g_{in}\varsigma, m_i, \delta_i) = \exp\left(-\frac{(g_{in}\varsigma - m_i)^2}{\delta_i^2}\right) \tag{20}$$

where m_i and δ_i are the center and width of the i-th hidden neuron, respectively.

Substituting Equation (18) into (12) yields

$$\dot{\varsigma} = \dot{g}_x - \dot{g}_y - \dot{u}_{nc} - \dot{u}_{sc} + \dot{w} + c_1\ddot{e} + c_2\dot{e} + c_3 e + c_4\int_0^t e(\tau)d\tau. \tag{21}$$

From Equations (14) and (21), it is obtained

$$\dot{\varsigma} = (\dot{u}_{dsmc} - \dot{u}_{nc} - \dot{u}_{sc}) + \dot{w} - W\mathrm{sgn}(\varsigma). \tag{22}$$

3.1. **Online learning algorithm.** The online learning algorithm is a gradient descent algorithm in the space of network parameters and aims at minimizing $\varsigma\dot{\varsigma}$ for achieving fast convergence of ς. Multiplying both sides of Equation (22) by ς gives

$$\varsigma\dot{\varsigma} = \varsigma[(\dot{u}_{dsmc} - \dot{u}_{nc} - \dot{u}_{sc}) + \dot{w} - W\mathrm{sgn}(\varsigma)]. \tag{23}$$

According to the gradient descent method, the learning rules are summarized as follows.

1) The weights α_i are updated by the following equation [29]

$$\Delta\alpha_i = -\eta_\alpha\frac{\partial\varsigma\dot{\varsigma}}{\partial\alpha_i} = -\eta_\alpha\frac{\partial\varsigma\dot{\varsigma}}{\partial\dot{u}_{nc}}\frac{\partial\dot{u}_{nc}}{\partial\alpha_i} = \eta_\alpha\varsigma g_{out}\theta_i \tag{24}$$

where $\Delta\alpha_i$ is the updated value of the i-th connection weights between the hidden layer and output layer and the positive constant η_α is the learning-rate parameter. The connective weights can be updated according to the following equation:

$$\alpha_i(t+1) = \alpha_i(t) + \Delta\alpha_i(t). \tag{25}$$

2) The center and width of the hidden neurons can also be adjusted in the following equations to increase the learning capability.

$$\Delta m_i = -\eta_m\frac{\partial\varsigma\dot{\varsigma}}{\partial m_i} = -\eta_m\frac{\partial\varsigma\dot{\varsigma}}{\partial\dot{u}_{nc}}\frac{\partial\dot{u}_{nc}}{\partial\theta_i}\frac{\partial\theta_i}{\partial m_i} = 2\eta_m\varsigma g_{out}\alpha_i\frac{(g_{in}\varsigma - m_i)}{\delta_i^2}\theta_i \tag{26}$$

$$\Delta\delta_i = -\eta_\delta\frac{\partial\varsigma\dot{\varsigma}}{\partial\delta_i} = -\eta_\delta\frac{\partial\varsigma\dot{\varsigma}}{\partial\dot{u}_{nc}}\frac{\partial\dot{u}_{nc}}{\partial\theta_i}\frac{\partial\theta_i}{\partial\delta_i} = 2\eta_\delta\varsigma g_{out}\alpha_i\frac{(g_{in}\varsigma - m_i)^2}{\delta_i^3}\theta_i \tag{27}$$

where Δm_i and $\Delta\delta_i$ are the updated values of the center and width for the i-th hidden neuron, respectively; and η_m and η_δ are the positive learning-rate parameters. The center and width of the hidden neurons are updated as follows:

$$m_i(t+1) = m_i(t) + \Delta m_i(t) \tag{28}$$

$$\delta_i(t+1) = \delta_i(t) + \Delta\delta_i(t). \tag{29}$$

3) The scaling factors of input and output variables also can be adjusted in the following equation to increase the learning capability.

$$\begin{aligned}\Delta g_{in} &= -\eta_{in}\frac{\partial \varsigma\dot{\varsigma}}{\partial g_{in}} = -\eta_{in}\frac{\partial \varsigma\dot{\varsigma}}{\partial \dot{u}_{nc}}\sum_{i=1}^{n}\frac{\partial \dot{u}_{nc}}{\partial \theta_i}\frac{\partial \theta_i}{\partial g_{in}} \\ &= -2\eta_{in}\varsigma^2 g_{out}\sum_{i=1}^{n}\left[\frac{(g_{in}\varsigma - m_i)}{\delta_i^2}\alpha_i\theta_i\right] \qquad (30)\end{aligned}$$

$$\Delta g_{out} = -\eta_{out}\frac{\partial \varsigma\dot{\varsigma}}{\partial g_{out}} = -\eta_{out}\frac{\partial \varsigma\dot{\varsigma}}{\partial \dot{u}_{nc}}\frac{\partial \dot{u}_{nc}}{\partial g_{out}} = \eta_{out}\varsigma\sum_{i=1}^{n}[\alpha_i\theta_i] \qquad (31)$$

where Δg_{in} and Δg_{out} are the updated values of the input and output scaling factors for the neuron network, respectively; and η_{in} and η_{out} are the positive learning-rate parameters. The scaling factors of input and output variables are updated as follows,

$$g_{in}(t+1) = g_{in}(t) + \Delta g_{in}(t) \qquad (32)$$

$$g_{out}(t+1) = g_{out}(t) + \Delta g_{out}(t). \qquad (33)$$

3.2. **Variable learning-rate parameters.** The learning algorithms (24), (26), (27), (30) and (31) call for a proper choice of the learning-rate parameters η_α, η_m, η_δ, η_{in} and η_{out}, respectively. For given small values of the learning-rate parameters, parameter convergence can be guaranteed but convergence speed is very slow. On the other hand, if the values of the learning-rate parameters are too large, the algorithm becomes unstable. To solve this problem, a variable learning rate is determined by considering a cost function as

$$E = \frac{1}{2}\varsigma^2. \qquad (34)$$

According to the gradient descent method, the adaptive law of the weight can be represented as [29]:

$$\Delta\alpha_i = -\eta_\alpha\frac{\partial E}{\partial \alpha_i} = -\eta_\alpha\frac{\partial E}{\partial \dot{u}_{nc}}\frac{\partial \dot{u}_{nc}}{\partial \alpha_i} = -\eta_\alpha\frac{\partial E}{\partial \dot{u}_{nc}}g_{out}\theta_i. \qquad (35)$$

If the plant dynamics is unknown, the Jacobian term cannot be obtained in advance. Therefore, the whole updating rules cannot work properly during the learning process. Lin and Peng [17] used a simple approximation of the error term $\dfrac{\partial E}{\partial \dot{u}_{nc}} = e + \dot{e}$. It could overcome the aforementioned problem and make the online learning possible; however, the stability analysis is not given. Yeh and Tsai [18] developed $\dfrac{\partial E}{\partial \dot{u}_{nc}} = \dfrac{\Delta e}{\Delta u}$ to make the approximation more accurate even though the plant dynamics is unknown; however, the algorithm is quite sensitive the external disturbances. In this paper, comparing Equation (24) with (35), the Jacobian term of the system can be found as $\dfrac{\partial E}{\partial \dot{u}_{nc}} = -\varsigma$. Then, the difference $\Delta\varsigma(t)$ associated with the dynamic sliding surface can be represented by

$$\varsigma(t+1) = \varsigma(t) + \Delta\varsigma(t) = \varsigma(t) + \left[\frac{\partial \varsigma(t)}{\partial \mathbf{P}}\right]^T \Delta\mathbf{P} \qquad (36)$$

where $\Delta\mathbf{P}$ denotes the change of an adjustable parameter vector, α_i in Equation (24), for example, in the updating rules (24), (26), (27), (30) and (31). Using the chain rule, we have

$$\frac{\partial \varsigma}{\partial \mathbf{P}} = \frac{\partial \varsigma}{\partial E}\frac{\partial E}{\partial \dot{u}_{nc}}\frac{\partial \dot{u}_{nc}}{\partial \mathbf{P}} = -\frac{\partial \dot{u}_{nc}}{\partial \mathbf{P}} \qquad (37)$$

and

$$\Delta \mathbf{P} = -\eta_{\mathbf{P}} \frac{\partial \varsigma \dot{\varsigma}}{\partial \mathbf{P}} = -\eta_{\mathbf{P}} \frac{\partial \varsigma \dot{\varsigma}}{\partial \dot{u}_{nc}} \frac{\partial \dot{u}_{nc}}{\partial \mathbf{P}} = \eta_{\mathbf{P}} \varsigma \frac{\partial \dot{u}_{nc}}{\partial \mathbf{P}}. \tag{38}$$

From Equations (37) and (38), it is obtained

$$\Delta \varsigma = \left[\frac{\partial \varsigma}{\partial \mathbf{P}}\right]^T \Delta \mathbf{P} = -\eta_{\mathbf{P}} \varsigma \left\| \frac{\partial \dot{u}_{nc}}{\partial \mathbf{P}} \right\|^2 \tag{39}$$

where $\|\cdot\|$ is the Euclidean norm. Consider a discrete-type Lyapunov function as

$$V_2 = \frac{1}{2}\varsigma^2(t). \tag{40}$$

The change in the Lyapunov function is expressed as

$$\begin{aligned} \Delta V_2 &= V_2(t+1) - V_2(t) = \frac{1}{2}\left[\varsigma^2(t+1) - \varsigma^2(t)\right] \\ &= \Delta\varsigma(t)\left[\varsigma(t) + \frac{1}{2}\Delta\varsigma(t)\right] \\ &= -\eta_{\mathbf{P}}\varsigma(t)\left\|\frac{\partial \dot{u}_{nc}}{\partial \mathbf{P}}\right\|^2 \left[\varsigma(t) - \frac{1}{2}\eta_{\mathbf{P}}\varsigma(t)\left\|\frac{\partial \dot{u}_{nc}}{\partial \mathbf{P}}\right\|^2\right] \\ &= \frac{1}{2}\eta_{\mathbf{P}}\varsigma^2(t)\left\|\frac{\partial \dot{u}_{nc}}{\partial \mathbf{P}}\right\|^2 \left[\eta_{\mathbf{P}}\left\|\frac{\partial \dot{u}_{nc}}{\partial \mathbf{P}}\right\|^2 - 2\right]. \end{aligned} \tag{41}$$

If $\eta_{\mathbf{P}}$ is chosen as $0 < \eta_{\mathbf{P}} < \dfrac{2}{\left\|\dfrac{\partial \dot{u}_{nc}}{\partial \mathbf{P}}\right\|^2}$, then the discrete-type Lyapunov stability is guaranteed due to $V_2 > 0$ and $\Delta V_2 < 0$. Therefore, the output tracking error will converge to zero as $t \to \infty$. In the following theorem, a sufficient condition on the variable learning-rate parameters is derived to ensure convergence of the output tracking error.

Theorem 3.1 (Connection Weights). *Let η_α be the learning-rate parameter of the adaptation law for the weights of the RBF network. Then, convergence of the tracking error is guaranteed if η_α is chosen as*

$$0 < \eta_\alpha < \frac{2}{n\left(|g_{out}|\,|\theta|_{\max}\right)^2} \tag{42}$$

where $|\theta|_{\max} = \max|\theta_i|$ and $|\cdot|$ is the absolute value.

Proof: Since

$$\frac{\partial \dot{u}_{nc}}{\partial \alpha_i} = g_{out}\theta_i \le |g_{out}\theta_i| \le |g_{out}|\,|\theta_i| \le |g_{out}|\,|\theta|_{\max} \tag{43}$$

and $\dfrac{\partial \dot{u}_{nc}}{\partial \alpha} = \left[\dfrac{\partial \dot{u}_{nc}}{\partial \alpha_1}, \dfrac{\partial \dot{u}_{nc}}{\partial \alpha_2}, ..., \dfrac{\partial \dot{u}_{nc}}{\partial \alpha_n}\right]^T$, it follows,

$$\left\|\frac{\partial \dot{u}_{nc}}{\partial \alpha}\right\| \le \sqrt{n}\,|g_{out}|\,|\theta|_{\max}. \tag{44}$$

From Equations (41) and (44), ΔV_2 can be rewritten as

$$\begin{aligned} \Delta V_2 &= \frac{1}{2}\eta_\alpha\varsigma^2\left\|\frac{\partial \dot{u}_{nc}}{\partial \alpha}\right\|^2\left[\eta_\alpha\left\|\frac{\partial \dot{u}_{nc}}{\partial \alpha}\right\|^2 - 2\right] \\ &\le \frac{1}{2}\eta_\alpha\varsigma^2 n\left(|g_{out}|\,|\theta|_{\max}\right)^2\left[\eta_\alpha n\left(|g_{out}|\,|\theta|_{\max}\right)^2 - 2\right]. \end{aligned} \tag{45}$$

If η_α is chosen as $0 < \eta_\alpha < \dfrac{2}{n\left(|g_{out}|\,|\theta|_{\max}\right)^2}$, then the discrete-type Lyapunov stability is guaranteed due to $V_2 > 0$ and $\Delta V_2 < 0$. So the output tracking error will converge to zero as $t \to \infty$. This completes the proof of Theorem 3.1.

Before presenting Theorem 3.2, we introduce the following lemmas [16]:

Lemma 3.1. *Let $f(r) = r\exp(-r^2)$, then $|f(r)| < 1, \forall r \in R$.*

Lemma 3.2. *Let $g(r) = r^2\exp(-r^2)$, then $|g(r)| < 1, \forall r \in R$.*

Theorem 3.2 (Center and Width). *Let η_m and η_δ be the learning-rate parameters of the adaptation laws for the center and width of the hidden neurons in the RBF network. The convergence of the tracking error is guaranteed if η_m and η_δ are chosen as*

$$0 < \eta_m, \quad \eta_\delta < \frac{|\delta|^2_{\min}}{2n(|\alpha|_{\max}\,|g_{out}|)^2} \tag{46}$$

where $|\alpha|_{\max} = \max|\alpha_i|$ and $|\delta|_{\min} = \min|\delta_i|$.

Proof: (a) According to Lemma 3.1, it follows

$$\left|\left[\frac{(g_{in}\varsigma - m_i)}{\delta_i}\right]\exp\left\{-\left[\frac{(g_{in}\varsigma - m_i)}{\delta_i}\right]^2\right\}\right| < 1.$$

Since

$$\begin{aligned}\frac{\partial \dot{u}_{nc}}{\partial m_i} &= \frac{\partial \dot{u}_{nc}}{\partial \theta_i}\frac{\partial \theta_i}{\partial m_i} = \frac{2\alpha_i g_{out}}{\delta_i}\frac{(g_{in}\varsigma - m_i)}{\delta_i}\theta_i \\ &\le \left|\frac{2\alpha_i g_{out}}{\delta_i}\frac{(g_{in}\varsigma - m_i)}{\delta_i}\theta_i\right| \\ &\le \left|\frac{2\alpha_i g_{out}}{\delta_i}\right|\left|\frac{(g_{in}\varsigma - m_i)}{\delta_i}\theta_i\right| \\ &< \left|\frac{2\alpha_i g_{out}}{\delta_i}\right| \le \frac{2\,|\alpha|_{\max}\,|g_{out}|}{|\delta|_{\min}}\end{aligned} \tag{47}$$

and $\dfrac{\partial \dot{u}_{nc}}{\partial \mathbf{m}} = \left[\dfrac{\partial \dot{u}_{nc}}{\partial m_1}, \dfrac{\partial \dot{u}_{nc}}{\partial m_2}, ..., \dfrac{\partial \dot{u}_{nc}}{\partial m_n}\right]^T$, we have

$$\left\|\frac{\partial \dot{u}_{nc}}{\partial \mathbf{m}}\right\| \le \sqrt{n}\frac{2\,|\alpha|_{\max}\,|g_{out}|}{|\delta|_{\min}}. \tag{48}$$

From Equations (41) and (48), ΔV_2 can be rewritten as

$$\begin{aligned}\Delta V_2 &= \frac{1}{2}\eta_m\varsigma^2\left\|\frac{\partial \dot{u}_{nc}}{\partial \mathbf{m}}\right\|^2\left[\eta_m\left\|\frac{\partial \dot{u}_{nc}}{\partial \mathbf{m}}\right\|^2 - 2\right] \\ &\le \frac{1}{2}\eta_m\varsigma^2 n\left(\frac{2\,|\alpha|_{\max}\,|g_{out}|}{|\delta|_{\min}}\right)^2\left[\eta_m n\left(\frac{2\,|\alpha|_{\max}\,|g_{out}|}{|\delta|_{\min}}\right)^2 - 2\right].\end{aligned} \tag{49}$$

If η_m is chosen as $0 < \eta_m < \dfrac{|\delta|^2_{\min}}{2n(|\alpha|_{\max}\,|g_{out}|)^2}$, then the discrete-type Lyapunov stability is guaranteed due to $V_2 > 0$ and $\Delta V_2 < 0$. Therefore, the convergence of the center in the hidden neurons is guaranteed.

(b) According to Lemma 3.2, one has

$$\left|\left[\frac{(g_{in}\varsigma - m_i)}{\delta_i}\right]^2\exp\left\{-\left[\frac{(g_{in}\varsigma - m_i)}{\delta_i}\right]^2\right\}\right| < 1.$$

Since

$$\begin{aligned}\frac{\partial \dot{u}_{nc}}{\partial \delta_i} &= \frac{\partial \dot{u}_{nc}}{\partial \theta_i}\frac{\partial \theta_i}{\partial \delta_i} = \frac{2\alpha_i g_{out}}{\delta_i}\frac{(g_{in}\varsigma - m_i)^2}{\delta_i^2}\theta_i \\ &\leq \left|\frac{2\alpha_i g_{out}}{\delta_i}\frac{(g_{in}\varsigma - m_i)^2}{\delta_i^2}\theta_i\right| \\ &\leq \left|\frac{2\alpha_i g_{out}}{\delta_i}\right|\left|\frac{(g_{in}\varsigma - m_i)^2}{\delta_i^2}\theta_i\right| \\ &< \left|\frac{2\alpha_i g_{out}}{\delta_i}\right| \leq \frac{2\left|\alpha\right|_{\max}\left|g_{out}\right|}{\left|\delta\right|_{\min}}\end{aligned} \tag{50}$$

and $\dfrac{\partial \dot{u}_{nc}}{\partial \boldsymbol{\delta}} = \left[\dfrac{\partial \dot{u}_{nc}}{\partial \delta_1}, \dfrac{\partial \dot{u}_{nc}}{\partial \delta_2}, ..., \dfrac{\partial \dot{u}_{nc}}{\partial \delta_n}\right]^T$, it can be obtained that

$$\left\|\frac{\partial \dot{u}_{nc}}{\partial \delta}\right\| \leq \sqrt{n}\frac{2\left|\alpha\right|_{\max}\left|g_{out}\right|}{\left|\delta\right|_{\min}}. \tag{51}$$

From Equations (41) and (51), ΔV_2 can be rewritten as

$$\begin{aligned}\Delta V_2 &= \frac{1}{2}\eta_\delta \varsigma^2 \left\|\frac{\partial \dot{u}_{nc}}{\partial \mathbf{m}}\right\|^2 \left[\eta_\delta \left\|\frac{\partial \dot{u}_{nc}}{\partial \mathbf{m}}\right\|^2 - 2\right] \\ &\leq \frac{1}{2}\eta_\delta \varsigma^2 n \left(\frac{2\left|\alpha\right|_{\max}\left|g_{out}\right|}{\left|\delta\right|_{\min}}\right)^2 \left[\eta_\delta n \left(\frac{2\left|\alpha\right|_{\max}\left|g_{out}\right|}{\left|\delta\right|_{\min}}\right)^2 - 2\right].\end{aligned} \tag{52}$$

If η_δ is chosen as $0 < \eta_\delta < \dfrac{\left|\delta\right|_{\min}^2}{2n(\left|\alpha\right|_{\max}\left|g_{out}\right|)^2}$, then the discrete-type Lyapunov stability is guaranteed due to $V_2 > 0$ and $\Delta V_2 < 0$. Therefore, the convergence of the width in the hidden neurons is guaranteed.

Theorem 3.3 (**Scaling Factors g_{in} and g_{out}**). *Let η_{in} and η_{out} be the learning-rate parameters of the adaptation laws for the scaling factors g_{in} and g_{out}, respectively. Then, convergence of the tracking error is guaranteed if η_{in} and η_{out} are chosen as*

$$0 < \eta_{in} < \frac{\left|\delta\right|_{\min}^2}{2(n\left|\alpha\right|_{\max}\left|g_{out}\right|\left|\varsigma\right|_{\max})^2} \tag{53}$$

and

$$0 < \eta_{out} < \frac{2}{(n\left|\alpha\right|_{\max}\left|\theta\right|_{\max})^2} \tag{54}$$

where $\left|\varsigma\right|_{\max} = \max\left|\varsigma\right|$.

Proof: (a) According to Lemma 3.1, it follows that

$$\left|\left[\frac{(g_{in}\varsigma - m_i)}{\delta_i}\right]\exp\left\{-\left[\frac{(g_{in}\varsigma - m_i)}{\delta_i}\right]^2\right\}\right| < 1.$$

Since

$$\begin{aligned}\frac{\partial \dot{u}_{nc}}{\partial g_{in}} &= g_{out}\sum_{i=1}^{n}\left[\frac{-2\alpha_i\varsigma}{\delta_i}\frac{(g_{in}\varsigma - m_i)}{\delta_i}\theta_i\right] \\ &\leq 2\left|g_{out}\right|\sum_{i=1}^{n}\left[\left|\frac{\alpha_i\varsigma}{\delta_i}\right|\left|\frac{(g_{in}\varsigma - m_i)}{\delta_i}\theta_i\right|\right] \\ &< 2\left|g_{out}\right|\sum_{i=1}^{n}\frac{\left|\alpha\right|_{\max}\left|\varsigma\right|}{\left|\delta\right|_{\min}} = \frac{2n\left|g_{out}\right|\left|\alpha\right|_{\max}\left|\varsigma\right|}{\left|\delta\right|_{\min}} \\ &\leq \frac{2n\left|g_{out}\right|\left|\alpha\right|_{\max}\left|\varsigma\right|_{\max}}{\left|\delta\right|_{\min}}\end{aligned} \tag{55}$$

we have

$$\left|\frac{\partial \dot{u}_{nc}}{\partial g_{in}}\right| \leq \frac{2n\left|g_{out}\right|\left|\alpha\right|_{\max}\left|\varsigma\right|_{\max}}{\left|\delta\right|_{\min}}. \tag{56}$$

From Equations (41) and (56), ΔV_2 can be rewritten as

$$\begin{aligned}\Delta V_2 &= \frac{1}{2}\eta_{in}\varsigma^2\left|\frac{\partial \dot{u}_{nc}}{\partial g_{in}}\right|^2\left[\eta_{in}\left|\frac{\partial \dot{u}_{nc}}{\partial g_{in}}\right|^2-2\right] \\ &\leq \frac{1}{2}\eta_{in}\varsigma^2\left(\frac{2n\left|g_{out}\right|\left|\alpha\right|_{\max}\left|\varsigma\right|_{\max}}{\left|\delta\right|_{\min}}\right)^2\left[\eta_{in}\left(\frac{2n\left|g_{out}\right|\left|\alpha\right|_{\max}\left|\varsigma\right|_{\max}}{\left|\delta\right|_{\min}}\right)^2-2\right].\end{aligned} \tag{57}$$

If η_{in} is chosen as $0<\eta_{in}<\dfrac{\left|\delta\right|_{\min}^2}{2(n\left|g_{out}\right|\left|\alpha\right|_{\max}\left|\varsigma\right|_{\max})^2}$, then the discrete-type Lyapunov stability is guaranteed due to $V_2>0$ and $\Delta V_2<0$. Therefore, the convergence of the scaling factor g_{in} is guaranteed.

(b) Since

$$\frac{\partial \dot{u}_{nc}}{\partial g_{out}}=\sum_{i=1}^{n}\alpha_i\theta_i\leq\sum_{i=1}^{n}\left|\alpha_i\right|\left|\theta_i\right|\leq\sum_{i=1}^{n}\left|\alpha\right|_{\max}\left|\theta\right|_{\max}=n\left|\alpha\right|_{\max}\left|\theta\right|_{\max} \tag{58}$$

we have

$$\left|\frac{\partial \dot{u}_{nc}}{\partial g_{out}}\right|\leq n\left|\alpha\right|_{\max}\left|\theta\right|_{\max}. \tag{59}$$

From Equations (41) and (59), ΔV_2 can be rewritten as

$$\begin{aligned}\Delta V_2 &= \frac{1}{2}\eta_{out}\varsigma^2\left|\frac{\partial \dot{u}_{nc}}{\partial g_{out}}\right|^2\left[\eta_{out}\left|\frac{\partial \dot{u}_{nc}}{\partial g_{out}}\right|^2-2\right] \\ &\leq \frac{1}{2}\eta_{out}\varsigma^2\left(n\left|\alpha\right|_{\max}\left|\theta\right|_{\max}\right)^2\left[\eta_{out}\left(n\left|\alpha\right|_{\max}\left|\theta\right|_{\max}\right)^2-2\right].\end{aligned} \tag{60}$$

If η_{out} is chosen as $0<\eta_{out}<\dfrac{2}{(n\left|\alpha\right|_{\max}\left|\theta\right|_{\max})^2}$, then the discrete-type Lyapunov stability is guaranteed due to $V_2>0$ and $\Delta V_2<0$. Therefore, the convergence of the scaling factor g_{out} is guaranteed.

3.3. **Switching compensator design.** There exists an approximation error between optimal neural controller and ideal DSMC system as

$$\dot{u}_{dsmc}=\dot{u}_{nc}^{*}+\varepsilon \tag{61}$$

where $\dot{u}_{nc}^{*}$ is the optimal neural controller and ε denotes the estimate approximation error and is assumed to be bounded as $0\leq\left|\varepsilon\right|\leq E$ with E is a positive constant. To ensure the stability of the closed-loop control system, this paper proposes a switching compensator as

$$\dot{u}_{sc}=\hat{E}\mathrm{sgn}(\varsigma) \tag{62}$$

where $\hat{E}$ denotes the estimated bound of the approximation error. Using Equations (61) and (62), Equation (22) can be rewritten as

$$\dot{\varsigma}=\varepsilon-\hat{E}\mathrm{sgn}(\varsigma)+\dot{w}-W\mathrm{sgn}(\varsigma). \tag{63}$$

For further analysis, define $\tilde{E}=E-\hat{E}$. To guarantee the stability of the ADSMNC system, a Lyapunov function candidate is defined as

$$V_3=\frac{1}{2}\varsigma^2+\frac{1}{2\eta_{\varepsilon}}\tilde{E}^2 \tag{64}$$

where η_ε is the learning rate. Differentiating Equation (64) with respect to time and using Equation (63), we can obtain

$$\begin{aligned} \dot{V}_3 &= \varsigma\dot{\varsigma} + \frac{1}{\eta_\varepsilon}\tilde{E}\dot{\tilde{E}} \\ &= \varsigma\left[\varepsilon - \hat{E}\mathrm{sgn}(\varsigma) + \dot{w} - W\mathrm{sgn}(\varsigma)\right] + \frac{1}{\eta_\varepsilon}\left(E - \hat{E}\right)\dot{\hat{E}}. \end{aligned} \tag{65}$$

For achieving $\dot{V}_3 \leq 0$, the adaptation law of the approximation error is designed as

$$\dot{\hat{E}} = \eta_\varepsilon |\varsigma| \tag{66}$$

so that Equation (65) can be rewritten as

$$\begin{aligned} \dot{V}_3 &= \varsigma\varepsilon - E|\varsigma| + \varsigma\dot{w} - W_{dsmc}|\varsigma| \\ &\leq |\varsigma||\varepsilon| - E|\varsigma| + |\varsigma||\dot{w}| - W|\varsigma| \\ &= |\varsigma|(|\varepsilon| - E) + |\varsigma|(|\dot{w}| - W) \leq 0. \end{aligned} \tag{67}$$

Since $\dot{V}_3$ is negative semi-definite, that is $V_3(s, \tilde{E}, t) \leq V_3(s, \tilde{E}, 0)$, it implies s and $\tilde{E}$ are bounded. Defining a function $\Omega(\tau) \equiv ks^2 \leq -\dot{V}_3$ and integrating $\Omega(t)$ with respect to time, it can be obtained that

$$\int_0^t \Omega(\tau)d\tau \leq V_3(s, \tilde{E}, t) - V_3(s, \tilde{E}, 0). \tag{68}$$

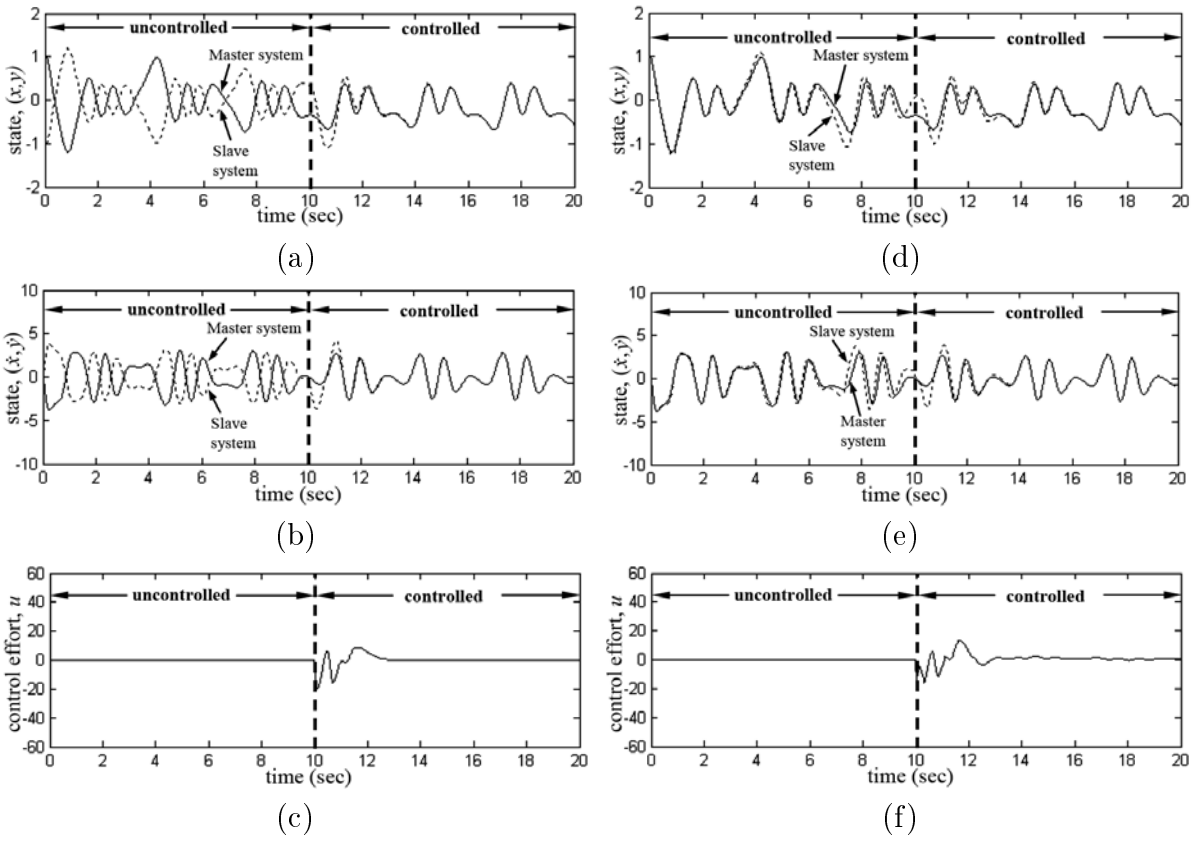

FIGURE 5. Simulation results of the fuzzy-rule-based control system [24]

Because $V_3(s, \tilde{E}, 0)$ is bounded, and $V_3(s, \tilde{E}, t)$ is nonincreasing and bounded, the following result can be obtained

$$\lim_{t\to\infty} \int_0^t \Omega(\tau) d\tau < \infty. \tag{69}$$

Moreover, since $\dot{\Omega}(t)$ is bounded, by Barbalat's Lemma [1], we can conclude that $\lim_{t\to\infty} \Omega(t) = 0$, i.e., $s \to 0$ as $t \to \infty$. As a result, the stability of the proposed ADSMNC system is guaranteed.

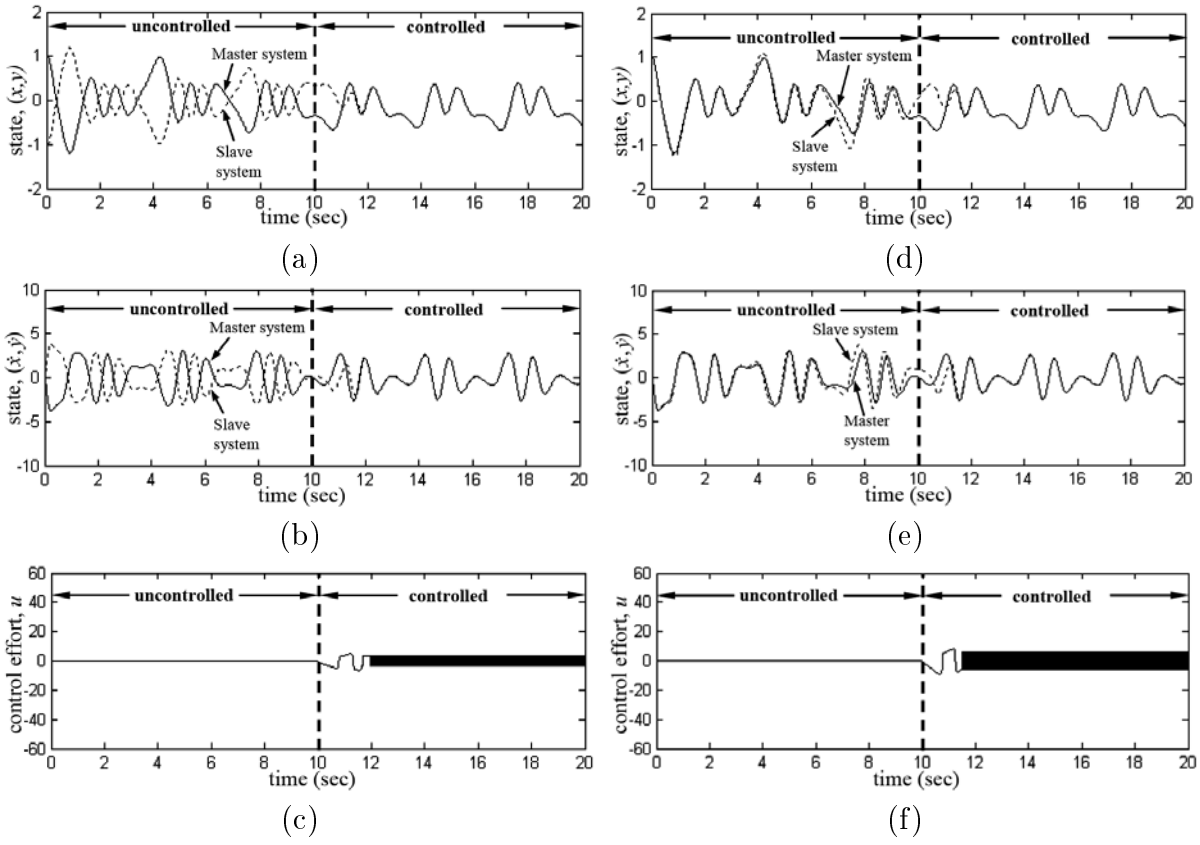

FIGURE 6. Simulation results of the adaptive fuzzy sliding-mode control system [25]

4. **Simulation Results.** In this section, the proposed ADSMNC system is applied to globally synchronize two identical chaotic gyros with nonlinear damping. To investigate the effectiveness of the proposed ADSMNC system, a comparison among the fuzzy-rule-based control [24], the adaptive fuzzy sliding-mode control [25] and the proposed ADSMNC is made. Two simulation cases including variations of parameters and initial condition are considered. The setting of Case 1 are $(x, \dot{x}, y, \dot{y}) = (1, 1, -1, -1)$, $f_x = 33$ and $f_y = 33$, and those of Case 2 are $(x, \dot{x}, y, \dot{y}) = (1, 1, 1, 1)$, $f_x = 33$ and $f_y = 36$.

4.1. **Comparison of different control methods.** First, the fuzzy-rule-based controller [24] is applied to synchronize two identical chaotic gyros with nonlinear damping. The fuzzy control rules are given in the following form,

$$\text{Rule } i : \text{IF } e \text{ is } F_1^i \text{ and } \dot{e} \text{ is } F_2^i, \text{ THEN } u \text{ is } f_i(e_1, e_2), \ i = 1, 2, \ldots, n \tag{70}$$

where, in the i-th rule, F_1^i and F_2^i are the fuzzy sets of e and $\dot{e}$, respectively, u is the output defined as the value of the analytical function $f_i(\cdot)$ with the input variables (e_1, e_2). The

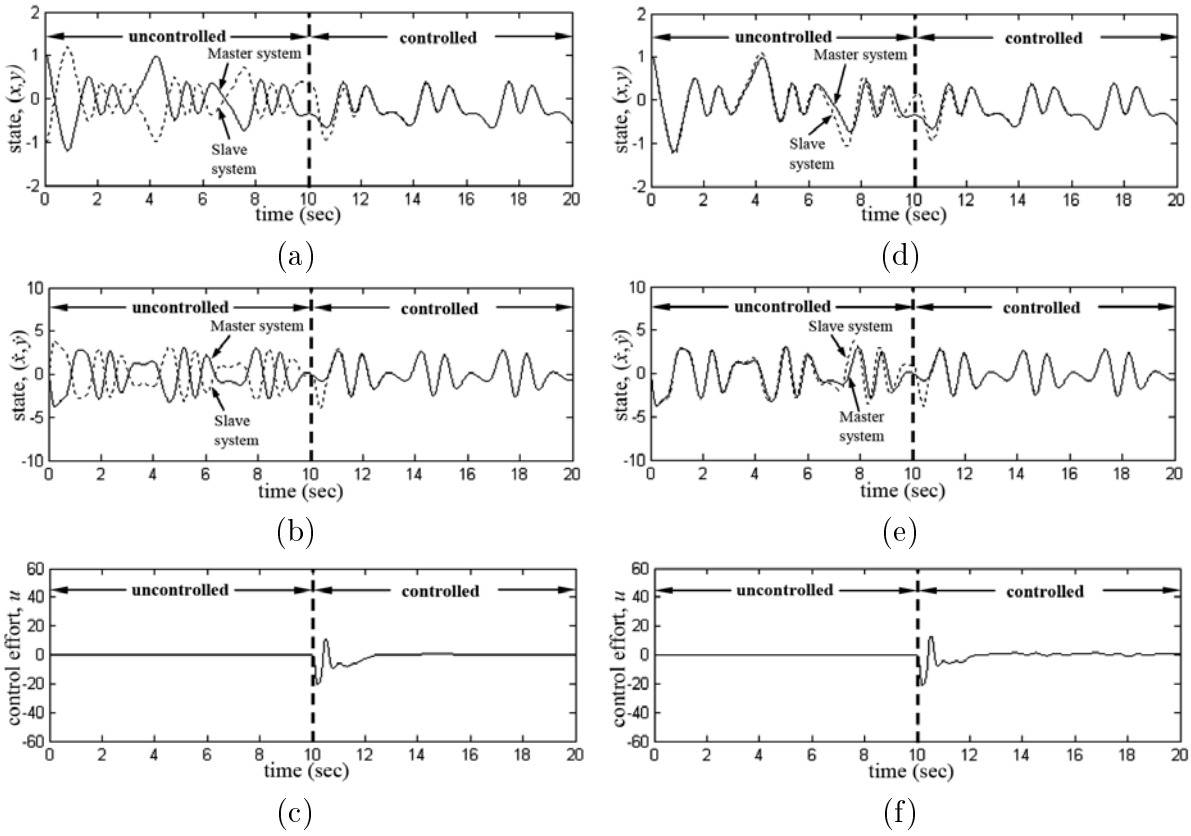

FIGURE 7. Simulation results of the proposed ADSMNC system

simulation results of the fuzzy-rule-based control system for Case 1 and Case 2 are shown in Figure 5. The tracking responses of states (x, y) are shown in Figures 5(a) and 5(d), the tracking responses of states $(\dot{x}, \dot{y})$ are shown in Figures 5(b) and 5(e), and the associated control efforts are shown in Figures 5(c) and 5(f). The simulation results show a favorable synchronization performance can be achieved. However, the fuzzy rules should be pre-constructed by a time-consuming trial-and-error tuning procedure to achieve the desired performance.

Then, the adaptive fuzzy sliding-mode control [25] is applied to synchronize two identical chaotic gyros again with a sliding surface being defined as $s = \dot{e} + 3e$. The adaptive fuzzy sliding-mode control requires the information of the bound of the lumped uncertainty. The simulation results of the adaptive fuzzy sliding-mode control system for Case 1 and Case 2 are shown in Figure 6. The tracking responses of states (x, y) are shown in Figures 6(a) and 6(d), the tracking responses of states $(\dot{x}, \dot{y})$ are shown in Figures 6(b) and 6(e), and the associated control efforts are shown in Figures 6(c) and 6(f). The simulation results show a favorable synchronization performance can be achieved under both the simulation cases after the controller parameters being well learned. Unfortunately, to guarantee the system stability, a switching compensator should be used, but the undesirable chattering phenomenon occurs as shown in Figures 6(c) and 6(f).

4.2. **ADSMNC system.** The ADSMNC system with variable learning rates is applied to synchronize two identical chaotic gyros with nonlinear damping. The control parameters of the proposed ADSMNC system are chosen as $a_1 = 8$, $a_2 = 16$, $b_1 = 2$, $b_2 = 1$ and $\eta_\varepsilon = 0.1$. The learning rates η_α, η_m, η_δ, η_{in} and η_{out} can be automatically tuned to suitable values using the proposed tuning algorithm. The simulation results of the ADSMNC system with variable learning rates for Case 1 and Case 2 are shown in Figure

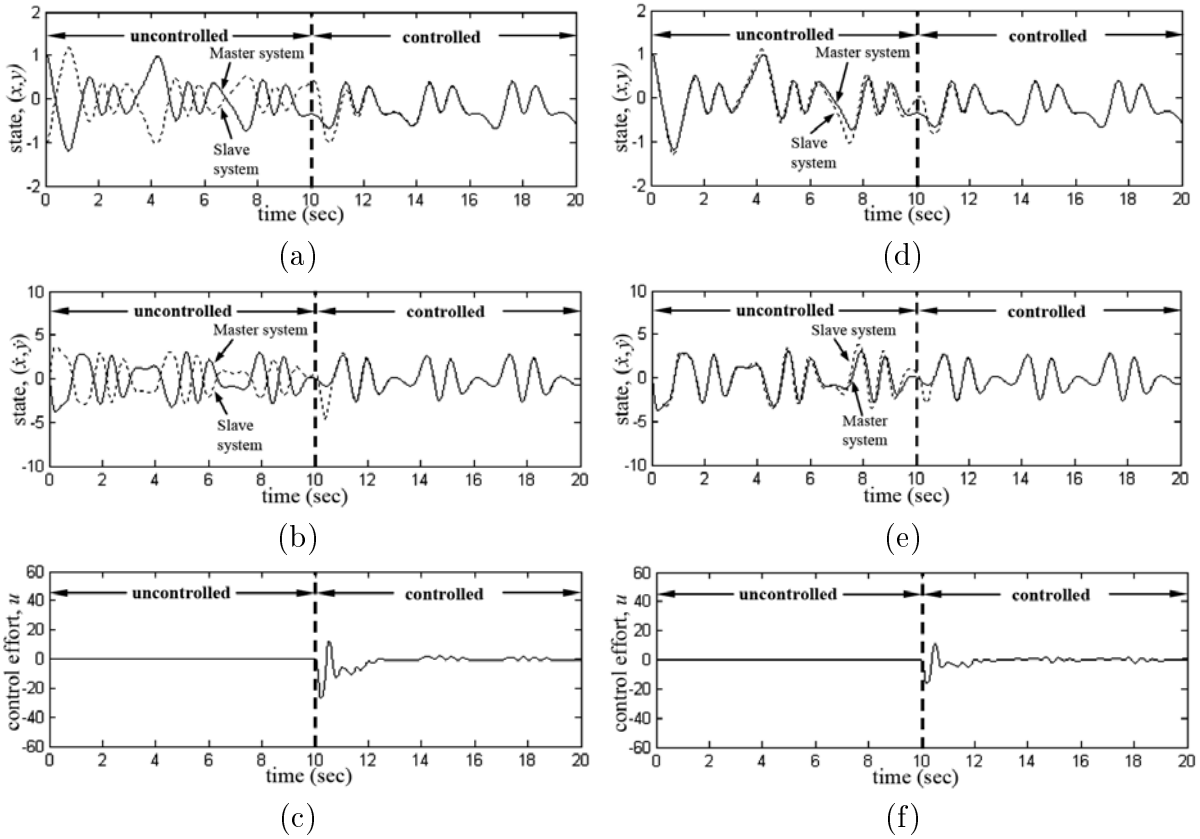

FIGURE 8. Simulation results of the proposed ADSMNC system for chaos synchronization with a coupling term

7. The tracking responses of states (x, y) are shown in Figures 7(a) and 7(d), the tracking responses of states $(\dot{x}, \dot{y})$ are shown in Figures 7(b) and 7(e), and the associated control efforts are shown in Figures 7(c) and 7(f). The simulation results show the proposed ADSMNC scheme with variable learning rates not only can achieve a favorable synchronization performance but also does not cause the chattering phenomena in the associated control efforts.

To demonstrate the robust performance of the proposed ADSMNC, a coupling term $F(\dot{x}, \dot{y}) = \cos(\dot{x} - 2\dot{y})$ is now added. The simulation results for Case 1 and Case 2 are shown in Figure 8. The tracking responses of states (x, y) are shown in Figures 8(a) and 8(d), the tracking responses of states $(\dot{x}, \dot{y})$ are shown in Figures 8(b) and 8(e), the associated control efforts are shown in Figures 8(c) and 8(f). The simulation results show not only perfect tracking can be achieved but also appropriate learning rates can be tuned because the proposed online learning algorithm is applied.

The selection of the learning-rate parameters (η_α, η_m, η_δ, η_{in} and η_{out}) for the online training of the RBF network has a significant effect on the network performance. The simulation results of the ADSMNC system with learning rates outside the convergence region for Case 1 and Case 2 are shown in Figure 9. The tracking responses of states (x, y) are shown in Figures 9(a) and 9(d), the tracking responses of states $(\dot{x}, \dot{y})$ are shown in Figures 9(b) and 9(e), and the associated control efforts are shown in Figures 9(c) and 9(f). The simulation results show the unstable tracking responses are induced due to the selection of learning rates outside the convergence region.

5. **Conclusions.** This paper has successfully demonstrated the design of an adaptive dynamic sliding-mode neural control (ADSMNC) system to synchronize two nonlinear

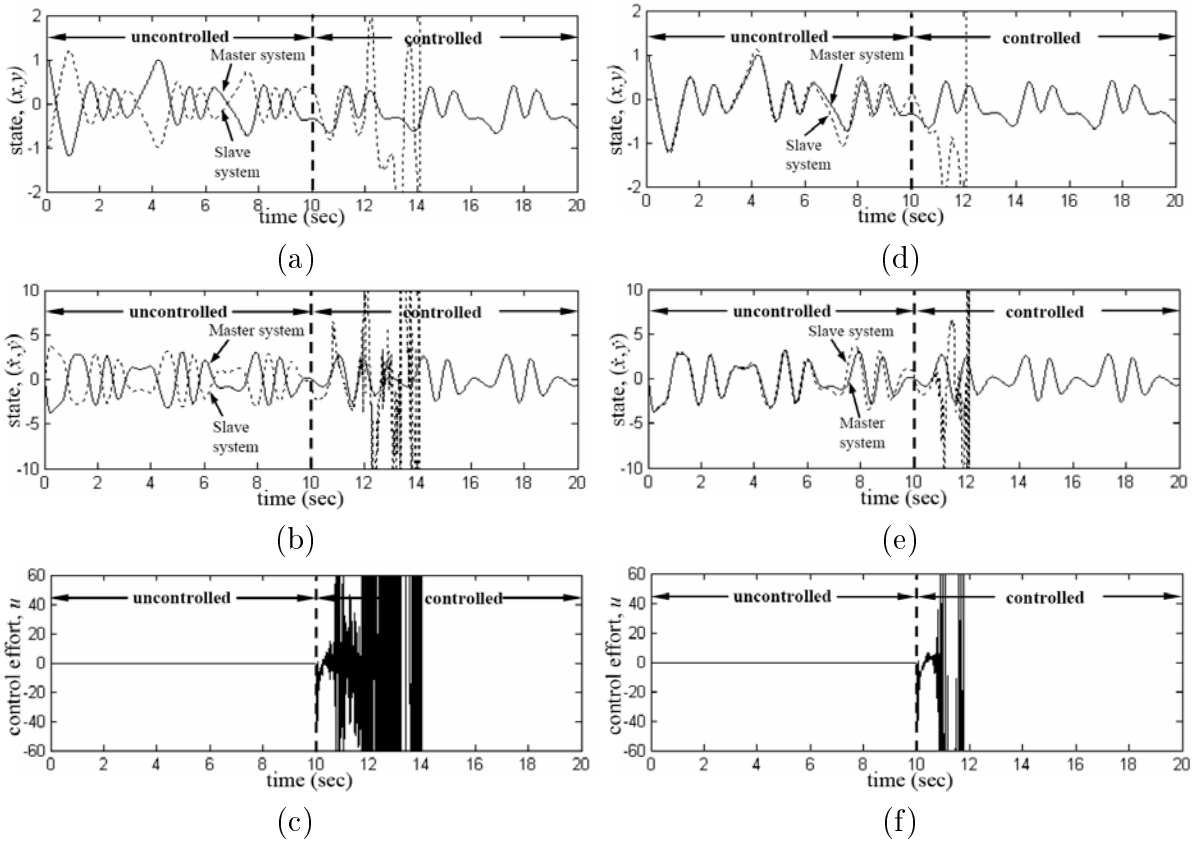

FIGURE 9. Simulation results of the ADSMNC system with learning rates outside the convergence region

identical chaotic gyros. The proposed ADSMNC system is composed of a neural controller and a switching compensator. The neural controller using a RBF network is the main controller, and the switching compensator is designed to dispel the approximation error introduced by the neural controller. To speed up the convergence of tracking errors, an analytical method based on a discrete-type Lyapunov function is proposed to determine the variable learning rates of the parameter adaptation laws. Finally, it is verified by the simulation study that system stabilization, favorable synchronization performance and no chattering phenomena can be achieved using the proposed ADSMNC system. Since the dynamic characteristic of chaotic gyros is nonlinear and the exact dynamic model is unobtainable, the developed model-free ADSMNC system is more suitable to drive the slave gyro system to synchronize the master gyro system.

Acknowledgment. The authors appreciate the partial financial support from the National Science Council of Taiwan under grant NSC 98-2221-E-216-040. The authors are grateful to the associate editor and reviewers for their valuable comments.

REFERENCES

[1] J. J. E. Slotine and W. Li, *Applied Nonlinear Control*, Englewood Cliffs, Prentice Hall, NJ, USA, 1991.

[2] V. I. Utkin, *Sliding Modes and Theirs Applications in Variable Structure Systems*, MIR Editors, Moscow, 1978.

[3] Z. Wang, S. Li and S. Fei, Finite-time tracking control of bank-to-turn missiles using terminal sliding mode, *ICIC Express Letters*, vol.3, no.4(B), pp.1373-1380, 2009.

[4] V. Parra-Vega, S. Arimoto, Y. H. Liu, G. Hirzinger and P. Akella, Dynamic sliding PID control for tracking of robot manipulators: Theory and experiments, *IEEE Transactions on Robotics and Automation*, vol.19, no.6, pp.967-976, 2003.

[5] A. J. Koshkouei, K. J. Burnham and A. S. I. Zinober, Dynamic sliding mode control design, *IEE Proc. of Control Theory and Applications*, vol.152, pp.392-396, 2005.

[6] C.-M. Lin and C.-F. Hsu, Neural network hybrid control for antilock braking systems, *IEEE Trans. Neural Netw.*, vol.14, no.2, pp.351-359, 2003.

[7] F.-H. Hsiao, J.-D. Hwang, C.-W. Chen and Z.-R. Tsai, Robust stabilization of nonlinear multiple time-delay large-scale systems via decentralized fuzzy control, *IEEE Trans. Fuzzy Syst.*, vol.13, pp.152-163, 2005.

[8] C.-C. Tsai, M.-B. Chen and S.-C. Lin, Robust tracking control for a wheeled mobile manipulator with dual arms using hybrid sliding-mode neural network, *Asian J. Control*, vol.9, pp.377-389, 2007.

[9] C.-F. Hsu, Self-organizing adaptive fuzzy neural control for a class of nonlinear systems, *IEEE Trans. Neural Netw.*, vol.18, pp.1232-1241, 2007.

[10] C.-F. Hsu, Intelligent position tracking control for LCM drive using stable online self-constructing recurrent neural network controller with bound architecture, *Control Eng. Pract.*, vol.17, pp.714-722, 2009.

[11] W. Xue and Y. Guo, Fuzzy neural network control in main steam temperature system, *ICIC Express Letters*, vol.3, no.3(A), pp.409-414, 2009.

[12] J. Liu, W. Wang, Q. Xiao and Z. Yang, Fault diagnosis for flight control system of unmanned aerial vehicle using fuzzy petri net, *ICIC Express Letters*, vol.4, no.4, pp.1319-1324, 2010.

[13] S. Kumarawadu and T.-T. Lee, Neuroadaptive combined lateral and longitudinal control of highway vehicles using RBF networks, *IEEE Trans. Intell. Transp. Syst.*, vol.7, no.4, pp.500-512, 2006.

[14] S. Wang and D. L. Yu, Adaptive RBF network for parameter estimation and stable air-fuel ratio control, *Neural Netw.*, vol.21, no.1, pp.102-112, 2008.

[15] Y. Yang and X. Wang, Adaptive H^{∞} tracking control for a class of uncertain nonlinear systems using radial-basis-function neural networks, *Neurocomputing*, vol.70, no.4-6, pp.932-941, 2007.

[16] T. Zhao, RBFN-based decentralized adaptive control of a class of large-scale non-affine nonlinear systems, *Neural Computing and Applications*, vol.17, pp.357-364, 2008.

[17] C.-M. Lin and Y.-F. Peng, Adaptive CMAC-based supervisory control for uncertain nonlinear systems, *IEEE Trans. Syst., Man, and Cybern., Part B: Cybern.*, vol.34, no.2, pp.1248-1260, 2004.

[18] M.-F. Yeh and C.-H. Tsai, Standalone CMAC control system with online learning ability, *IEEE Trans. Syst., Man, and Cybern., Part B: Cybern.*, vol.40, no.1, pp.43-53, 2010.

[19] R.-J. Wai and C.-H. Tu, Development of Lyapunov-based genetic algorithm control for linear piezoelectric ceramic motor drive, *IEEE Trans. Ind. Electron.*, vol.54, no.5, pp.2566-2582, 2007.

[20] F.-J. Lin, S.-Y. Chen, L.-T. Teng and H. Chu, Recurrent FL-based fuzzy neural network controller with improved particle swarm optimization for a linear synchronous motor drive, *IEEE Trans. Magn.*, vol.45, no.8, pp.3151-3165, 2009.

[21] H.-K. Chen, Chaos and chaos synchronization of a symmetric gyro with linear-plus-cubic damping, *J. Sound Vibr.*, vol.255, no.4, pp.719-740, 2002.

[22] K. B. Arman, F. Kia, P. Naser and L. Henry, A chaotic secure communication scheme using fractional chaotic systems based on an extended fractional Kalman filter, *Commun. Nonlinear Sci. Numer. Simulat.*, vol.14, pp.863-879, 2009.

[23] T. Xiang, K. W. Wong and X. Liao, An improved chaotic cryptosystem with external key, *Commun. Nonlinear Sci. Numer. Simulat.*, vol.13, no.9, pp.1879-1887, 2008.

[24] H.-T. Yau, Nonlinear rule-based controller for chaos synchronization of two gyros with linear-plus-cubic damping, *Chaos Solitons Fract.*, vol.34, no.4, pp.1357-1365, 2007.

[25] A. Poursamad and A. H. Davaie-Markazi, Robust adaptive fuzzy control of unknown chaotic systems, *Appl. Soft Comput.*, vol.9, pp.970-976, 2009.

[26] E. M. Elabbasy, H. N. Agiza and M. M. El-Dessoky, Adaptive synchronization of Lü system with uncertain parameters, *Chaos Solitons Fract.*, vol.21, pp.657-667, 2004.

[27] H. Salarieh and M. Shahrokhi, Indirect adaptive control of discrete chaotic systems, *Chaos Solitons Fract.*, vol.34, pp.1188-1201, 2007.

[28] S. Dadras and H. R. Momeni, Adaptive sliding mode control of chaotic dynamical systems with application to synchronization, *Math. Comput. in Simulat.*, vol.80, pp.2245-2257, 2010.

[29] C.-M. Lin and C.-F. Hsu, Supervisory recurrent fuzzy neural network control of wing rock for slender delta wings, *IEEE Trans. Fuzzy Syst.*, vol.12, pp.733-742, 2004.